Biochimica et Biophysica Acta, 1061 (1991) 39–48

 0005-2736/91/$03.50
ADONIS 000527369100056R

BBAMEM 75059

Detection of structural defects in phosphatidylcholine membranes by small-angle neutron scattering. The cluster model of a lipid bilayer

V.I. Gordeliy [1], V.G. Ivkov [2], Yu.M. Ostanevich [1] and L.S. Yaguzhinskij [3]

[1] *Joint Institute for Nuclear Research, Laboratory of Neutron Physics,* [2] *Institute of Biological Physics, Academy of Sciences of the U.S.S.R., Pushchino, Moscow Region and* [3] *Moscow State University, Moscow (U.S.S.R.)*

(Received 12 June 1990)

Key words: Membrane structure; Lipid bilayer; Phosphatidylcholine; Small angle neutron scattering

The oriented DPPC multilayers hydrated by D_2O have been studied by a small-angle neutron scattering method in the Guinier range, and the gyration radius of the structural inhomogeneities has been estimated at about 29 Å. They are interpreted as the annular defects between adjacent clusters uniting the all-*trans* chain 'segments' adjacent to the polar head group regions. The angle of the 'segment' tilt is determined by the hydrated polar group area (59.2 Å^2 for DPPC bilayers) and has been estimated to be about 44° under the given experimental conditions. The hydrocarbon interior of a bilayer can be suggested as a 'sandwich' that is formed by two clustered layers (approx. 7 Å of the thickness) and the central disordered (liquid) layer. The average cluster size along the bilayer surface is estimated to be approx. 24 Å which correlates with the estimations of the short order region dimensions from the halfwidth of the X-ray 'packing' reflex (4.6 Å)$^{-1}$. The average interchain separation of approx. 5 Å and the average cross-section area of a chain in a cluster (21.4 Å^2) were estimated from the reflex position and the chain cross-section geometry. The total volume of defects and the fraction of a bilayer surface occupied by them were estimated too.

Introduction

A 'liquid' lipid bilayer is a structural basis of all biological membranes which determines the barrier properties [1]. Lipid bilayers formed from extracted and synthetic lipids are widely used to study some membrane processes such as a passive transport of molecules and ions, phase transitions, a partition of chemicals between aqueous and membrane phases. Average conformations and dynamics of lipid molecules in bilayers are well-characterized by numerous physical-chemical methods [2–27], but molecule arrangements and interactions are the subjects of discussion.

Stewart in 1928 proposed the existence of 'cytotactic groups' (clusters) of molecules in liquid paraffins to explain X-ray diffraction pictures [28]. Segerman [29] was apparently one of the first who postulated lipid clusters in biological membranes and estimated their dimensions along a bilayer plane from the X-ray peak width. For erythrocyte 'ghosts' the average cluster diameter was estimated to be approx. 24 Å [29]. In 1972 Levine wrote in his critical review [17] that "the sharpness of the diffraction peak given by the perpendicular chains indicates that the hydrocarbon core contains regions, probably near the water/hydrocarbon interface, where almost fully extended chains lie with their axes parallel and are packed in fairly large groups... Unfortunately it was not possible to analyse the problem rigorously".

Two years after Lee et al. [30] supposed the liquid cluster existence in dioleoylphosphatidylcholine bilayers to explain the deviations from linear Arrhenius behaviour of ESR spin-probes. An analogous interpretation was used for fluorescence polarization data [16], where authors suggested that the probe was segregating into relativley small regions of the bilayer by its exclusion from 'liquid clusters'. Clusters in a physical-chem-

Abbreviations: DPPC, dipalmitoylphosphatidylcholine; DMPC, dimyristoylphosphatidylcholine; EPC, egg yolk phosphatidylcholine; NMR, nuclear magnetic resonance; ESR, electron spin resonance; RH, relative humidity; FWHM, full width at half-maximum

Correspondence: V.I. Gordeliy, Laboratory of Neutron Physics, Joint Institute for Nuclear Research, 101000 Moscow, Box 79, U.S.S.R.

ical sense can be represented as "...short-lived more densely packed arrangements of molecules within the environment of freely dispersed molecules" [30]. We will restrict the following analysis to the hydrocarbon bilayer interior because we have no methods to determine the real polar group arrangements.

A cluster model predicts essentially the existence of short-lived defects of the molecular arrangement between adjacent clusters [31,32]. Two kinds of dynamic defect, 'i-defects' at a membrane/water interface and 'm-defects' in a bilayer hydrocarbon interior, have been suggested [33] to explain transmembrane motion processes. A geometry of these defects is unknown. First propositions about defect geometry were made by Träube [34] in his 'kink' model. This model describes a water transport as a result of the *gauche-trans-gauche* conformer motion along hydrocarbon chains preferentially oriented along the normal to a bilayer surface. Recent investigations show that this model is not in accordance with the physical properties of a fluid lipid bilayer [20,22], although some contribution of kinks takes place.

The semiquantitative cluster model of a 'liquid' PC (lecithin) bilayer was suggested in 1982 [15]. The average interchain distance in clusters [14,15], the average cluster dimensions along and across a bilayer [15,35], the real area of hydrated polar head groups at a bilayer surface [36], the probable geometry, sizes and apparent free energy of defects [15,36] have been estimated in the frames of this model. The statistical-mechanical calculations of entropy changes at a gel-liquid crystal phase transition also gave satisfactory results for a cluster model [37].

It is obvious that any structural model of a liquid lipid bilayer must base on the ground of some distinct experimental facts. The main facts are following: (1) the partial specific volume of a 'liquid' bilayer is only 2–4% more than that for a solid one [38–40]; (2) the characteristic 'plateau' for the ^{13}C- and ^{2}H-NMR order parameter and relaxation time profiles along hydrocarbon chains [5–9,11,18–22,41–50]; (3) the position and the width of the X-ray and neutron 'packing' reflex $(4.6\ \text{Å})^{-1}$ from fluid hydrocarbon chains [11,14,15, 17,35,51–53]; (4) the positions of CH_2-groups of hydrocarbon chains with respect to the bilayer centre [4,27]; (5) the length of all-*trans* segments of hydrocarbon chains for series of lecithins [54]; (6) the axial symmetry of the acyl chain motion with respect to the normal to the bilayer surface [20,22]. Also, other experimental data must not contradict the model.

We made an attempt to measure the average dimensions and concentration of the chain arrangement inhomogeneities in 'liquid' dipalmitoylphosphatidylcholine bilayers along a bilayer plane by a low-angle neutron scattering method. These dimensions were compared with those estimated from the X-ray 'packing' reflex width and the data were analysed in the frames of a cluster model for molecular arrangements in a 'liquid' lipid bilayer.

Materials and Methods

Dipalmitoylphosphatidylcholine (Serva) oriented multibilayers were prepared analogously to Ref. 55. 10% solution of DPPC in ethanol was put on the quartz glass plate (24×24 mm^2) and dried at 70°C. The slow annealing procedure [56] gave highly ordered samples (the FWHM of the rocking curve was about 2°). The dry weight of the lipid for each of three samples used was 50 ± 3 mg.

The samples were placed into a hermetic quartz glass container with a suitable salt solution or dehumidifier on the bottom. Aqueous K_2SO_4 solution (RH ≅ 97%) and P_2O_5 (RH ≅ 0%) were used for these goals. The sample equilibration was examined for more than 2 h. The lipid chain phase state was examined from a diffraction maxima positions: $(4.2\ \text{Å})^{-1}$ for the $L_{\beta'}$ phase and $(4.6\ \text{Å})^{-1}$ for the L_α phase [14,17]. Measurements were carried out at two temperatures: 23°C ($L_{\beta'}$) and 55°C (L_α).

Neutron scattering measurements were made on the time-of-flight small-angle scattering spectrometer at IBR-2 pulsed reactor [57]. The incoming neutron beam parallel to the plane of the quartz plate was collimated to the 22 mm diameter in the direction perpendicular to the sample surface (Fig. 1). The mean thermal neutron flux in the sample position was $3.2 \cdot 10^7\ \text{cm}^{-2} \cdot \text{s}^{-1}$. The sample-detector distance was 10.63 m and the range of the observed scattering vector lengths was $0.02 < q < 0.4$ Å^{-1} ($q = (4\pi/\lambda)\sin(\theta/2)$), where θ is the scattering angle and λ is the wavelength). Metallic vanadium was used as a standard scatterer (measurements were bound with standard every 5 min). The whole experiment for one sample was being continued for about 10 h. The excess neutron scattering along the bilayer plane at the multibilayer hydration was determined. This allowed correction of measurement results for the instrument background, the cuvette scattering and the 'dry' lipid scattering.

Extrapolation of the scattered intensity to the zero scattering vector length gives the apparent forward scattered intensity per unit volume of the sample $I(0)$, which depends on the inhomogeneity parameters [58]:

$$I(0) \approx I_0 n V^2 (\rho - \rho_S)^2 \qquad (1)$$

where I_0 is the incoming beam intensity, n is the number of inhomogeneities per unit volume of the sample, V is the volume of a single inhomogeneity and $\rho - \rho_S$ is the difference of the scattering length densities of the inhomogeneity and of its surrounding. This difference is often called a contrast.

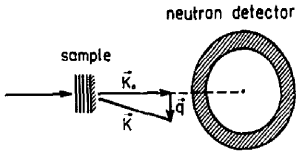

Fig. 1. The scheme of the experiment.

Eqn. 1 is a reasonable approximation at $nV \ll 1$ and it allows one to estimate n, if $I(0)$ is adequately compared * with I_0 and $V^2(\rho - \rho_s)^2$ is calculated from the model parameters and a gyration radius, R_g. The latter can be determined from the slope of ln $I(q)$ vs. q^2 plot (the so-called Guinier plot).

For the oriented multilayers and scattering vector directed along the bilayer surface:

$$I(q) = I(0)\exp(-q^2R_g^2/2) \tag{2}$$

The R_g value allows one to calculate V if inhomogeneity geometry is assumed from any independent experimental data.

R_g is determined by the spatial distribution of the scattering length density [59]:

$$R_g^2 = \int_v (\rho(\vec{r}) - \rho_S) r^2 \, dv \Big/ \int_v (\rho(\vec{r}) - \rho_S) \, dv \tag{3}$$

where $\vec{r}$ is a radius vector, ρ_S is the bulk scattering length density, the integration is made over the sample, volume, the origin is taken in the centre of "mass" $(\rho - \rho_S)$.

Results

The dependence of the excess scattering intensity (with respect to 'dry' multilayers) on the square of the scattering vector is shown in Fig. 2. For the solid bilayers the excess intensity is practically zero. Thus the hydration of 'liquid' bilayers gives the well detectable scattering parallel to the bilayer plane. It is reasonable to suppose that this effect is a result of water penetration into the dynamic structural defects in a fluid bilayer.

The excess intensity in the Guinier coordinates is shown in Fig. 3. It is well described by the Guinier approximation (Eqn. 2) allowing determination of two scatterer parameters, $I(0)$ and R_g. These values calculated by the least-squares method are shown in Table I for three samples. The R_g values correlate with each other sufficiently well (in the limit of errors) while the intensity data are more dispersed. The latter may be a result of the inexactitudes in the lipid weight determination.

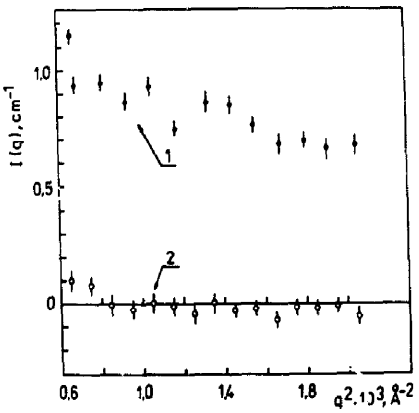

Fig. 2. The excess intensity of the small-angle neutron scattering (at multilayer hydration by D_2O) in dependence on q^2 ($q = (4\pi/\lambda)\cdot\sin(\theta/2)$). The sample N2 - 8.7 mg·cm^{-2} of multilamellar DPPC structure: 1, L_α phase; 2, $L_{\beta'}$ phase.

To calculate other parameters it is necessary to know the contrast value. It depends on the kind of radiation used (X rays, neutrons or electrons) and in the case of neutrons, on the isotope composition of a sample. The ^1H to ^2H substitution increases greatly the contrast for neutrons. Supposing the defects in a bilayer are empty or filled with ^2H_2O, the ratio of the squared contrast for neutrons and X-rays can be easily calculated [58]; the results are given in Table II.

To calculate the total defect concentration, n, from $I(0)$ values the inhomogeneity (defect) volume, V, must be determined from the chosen structural model. For

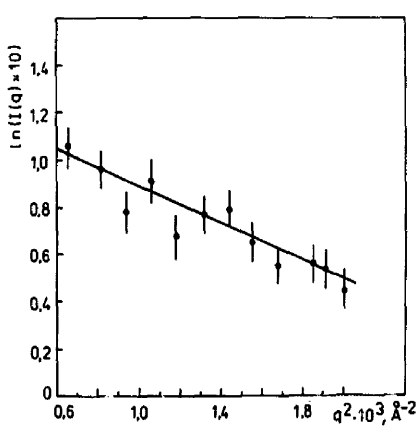

Fig. 3. The excess intensity of the small-angle neutron scattering in Guinier approximation. The sample N2, D_2O, RH = 97%, 55 °C, L_α phase.

* The scattering cross-section is put on to absolute scale.

TABLE I

Scatterer parameters

Sample	$I(0)$ (cm^{-1})	R_g (Å)	χ^2 per degree of freedom
N1	0.48±0.06	29.8±2.6	1.1
N2	0.34±0.01	29.7±6.9	0.5
N3	0.36±0.04	26.7±3.8	0.8
Weighted average values for three samples	0.36±0.04	29 ±2	

TABLE II

The calculated ratio of the scattering intensities by the defects in the lipid bilayers for neutrons and X-rays [59]

Medium	Defect filling	$(\rho-\rho_S)^2\cdot10^{-20}$ (cm^{-4})		Ratio of intensities neutrons/ X rays
		neutrons	X rays	
Hydrocarbon chains	D_2O	45.2	1.44	31.4
	empty	0.116	67.0	$1.7\cdot10^{-3}$
Polar head groups	D_2O	20.8	12.9	1.62
	empty	3.24	169.0	$1.9\cdot10^{-2}$

the following calculation it is necessary to know the repeat distance value (lamellar spacing), d, which depends on the temperature and relative humidity values. At 55°C and RH = 97%, d = 54 Å, which is close to 54.1 Å in Ref. 27 for DPPC bilayers at 50°C and 25

TABLE III

The calculated parameters of the porous membrane

Pore parameters	Formula	Value
Length	l_h	30 Å
Radius	$R_p=\sqrt{2}R_g$	41 Å
Area	$S_p=\pi R_p^2$	$5.3\cdot10^3$ Å^2
Volume	$V_p=S_p l_h$	$1.6\cdot10^5$ Å^3
Concentration in the sample volume	$n_p=\dfrac{I(0)}{(\rho-\rho_S)^2V_p^2}$	$2.9\cdot10^{15}$ cm^{-3}
Total fraction of volume occupied by pores	$\alpha_V=n_pV_p$	$4.6\cdot10^{-4}$
Number of pores per 1 cm^2 of a bilayer	$n_S=n_pd$	$1.55\cdot10^9$
Total area fraction occupied by pores	$\alpha_S=n_SS_p$	$8.2\cdot10^{-4}$

wt% H_2O. The latter corresponds to about 13.5 H_2O molecules per DPPC (molecular mass is 733). AT RH = 97%, 'liquid' EPC bilayers (22°C) absorb about 14 H_2O molecules per lipid molecule [60]. Similar conditions in the present work and that in Refs. 4 and 27 allow one to use the data of Refs. 4 and 27 for model descriptions.

Discussion

There are two reliable kinds of defects with the measured gyration radius in a liquid lipid bilayer, aqueous pores through the whole bilayer interior and annular defects at the boundary of the polar and hydrocarbon regions. It is difficult to invent something different.

The model of the porous membrane

This is the simplest model supposing the defects are through cylindrical holes filled with water. The defects of the aqueous pore type in membranes were suggested to explain their high permeabilities for water [61,62]. This is an alternative to the 'kink' model. The hydrocarbon layer thickness (the cylinder length), $l_h \cong 30$ Å, according to Refs. 4 and 27 and the cylinder radius is $R_g\sqrt{2}$. The cylinder volume is about $1.6\cdot10^{-19}$ cm^3. Other parameters of this model can be calculated from Eqn. 1 and data of Table II. They are given in Table III. Thus three values, R_g, $I(0)$ and V, were obtained from our own experiments, $(\rho-\rho_S)^2$ was calculated from general scatterer properties and only l_h was assumed based on the data of Refs. 4 and 27.

The pore diameter is large enough to take the diffusion coefficient, D, similar to that in water. Then the membrane permeability for water [63–65]:

$$P=\alpha_S\frac{D}{l_h} \tag{4}$$

where $D=5.02\cdot10^{-5}$ $cm^2\cdot s^{-1}$ at 50°C and $2.5\cdot10^{-5}$ $cm^2\cdot s^{-1}$ at 25°C [66]. The experimentally determined water permeability of the EPC bilayers is about $8\cdot10^{-3}$ $cm\cdot s^{-1}$ at 37°C and $4.5\cdot10^{-3}$ $cm\cdot s^{-1}$ at 25°C (large vesicles) or $1.7\cdot10^{-3}$ $cm\cdot s^{-1}$ at 44°C (small vesicles) [67]. The substitution of D values and the parameters from Table III into the Eqn. 4 gives approx. $160\cdot10^{-3}$ $cm\cdot s^{-1}$ (50°C) or approx. $80\cdot10^{-3}$ $cm\cdot s^{-1}$ (25°C). Yet more discrepancies are obtained for small ions. If the diffusion coefficient is 10^{-5}–10^{-6} $cm^2\cdot s^{-1}$ [63] the respective permeabilities are $2.7\cdot10^{-2}$–$2.7\cdot10^{-3}$ $cm\cdot s^{-1}$. The experimental values are approx. 10^{-8} $cm\cdot s^{-1}$ according to electrical measurements or approx. 10^{-6} $cm\cdot s^{-1}$ according to isotopic data [63].

Thus the detected inhomogeneities can not obviously be due to the cylindrical water pores piercing a membrane.

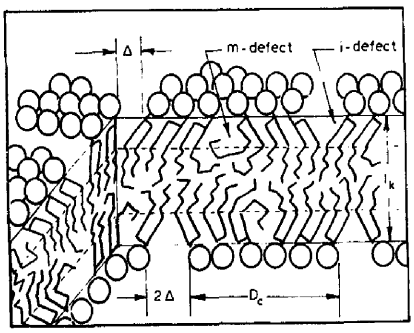

Fig. 4. Schematic picture of lipid molecule arrangements in a liquid lipid bilayer.

The cluster model

The alternative assumption is that neutrons are scattered by 'D_2O-contrasted' defects between the adjacent clusters [15]. A defect configuration and location in a 'liquid' bilayer is determined by cluster geometry. It is obvious that this model must be built on the basis of the totality of distinct experimental facts that do not depend on interpretation. The main facts, in our opinion, are enumerated in the Introduction. They can be explained supposing a three-layer 'sandwich' organization of a lipid bilayer where all-*trans* chain 'segments', adjacent to the polar head groups, are united into clusters, and the more disordered central layer is similar to liquid hydrocarbons (Fig. 4). The axial symmetry of the chain motion is apparently a results of both the whole clustered molecule groups rotation and lipid molecule diffusion between adjacent clusters.

Similar 'three-layer' structural organization of a bilayer hydrocarbon interior, where two 'ordered' layers are divided by the 'disordered' layer in the bilayer center, was suggested in Ref. 2 exclusively on the basis of the structural features of lipid molecules. The similar hypothesis has been assumed in Ref. 68 from the analysis of the solubility of chain molecules in membranes and in Ref. 69 for the black film conductivity.

Geometry of defects

If the measured scatterers are not the aqueous pores it is reasonable to suppose that the annular defects at a bilayer interface give the detectable neutron scattering parallel to the bilayer plane. The geometry of defects is schematically shown in Fig. 4. Similar to Ref. 33 we mark them as i-defects (interfaciai) and m-defects (defects of a hydrocarbon matrix). The latter are probably 'filled' in the main due to the flexible chains, but can also entrap some molecules and ions.

Defect form and dimensions are determined by the length of all-*trans* 'segments' and their tilting angle. The effective length of an all-*trans* segment of a lipid chain can be estimated at first from NMR data [6–8,19–22,44,49,70], where a similar order parameter and spin-lattice relaxation time, T_1, are observed for C3-C9 methylene groups. Independently this value has been determined by Vogel and Jahnig [54] by the Raman spectroscopy method. For the series of synthetic phosphatidylcholines it was equal to about 8 CH_2-groups (approx. 10 Å); for liquid DMPC, for example, $N_{all\text{-}t} \cong$ 7.6 methylene groups [54]. The theoretical calculations [70–73] also show preferentially *trans* conformations for the CH_2-groups adjacent to the polar regions, although authors initially do not assume tilting of the collective chain.

The correct quantitative estimations of the chain tilting against the normal to a bilayer surface have been obtained from neutron diffraction data [4,27]. Fig. 5 shows the dependence of the average distances of deuterium labeled CH_2-groups from the bilayer centre on their positions in acyl chains for DPPC liquid bilayers. The linear plot allows calculation of the distance increment on the CH_2-group, $\Delta d_{CH_2} = 0.9$ Å, and the angle of the tilt about the normal is $\phi = \arccos(0.9/1.25) = \arccos 0.72 \cong 44°$ (1.25 Å is the 'length of CH_2-link', i.e., the length of the C–C bond projection on the long axis of the hydrocarbon chain in the all-*trans* conformation). The small width (approx. 1.5 Å) of the peaks characterizing the deuterium label location in a bilayer [27] shows that just the segment tilt but not the simple chain flexibility takes place in this case.

Petersen and Chan [49] attempted to explain the ^{2}H-NMR order parameter profile also by the motion of an all-*trans* segment tilted to the axis normal to the bilayer surface. The angle of the chain tilting was estimated at approx. 30–47° for EPC bilayers by the ESR spin-label method [74–76]. It must be noted that the molecule conformation pictured in Fig. 4 was proposed first in Ref. 76 and was used in Ref. 77 to describe molecular arrangement in lipid monolayers at oil/water interfaces. However, the distortions of a bilayer due to

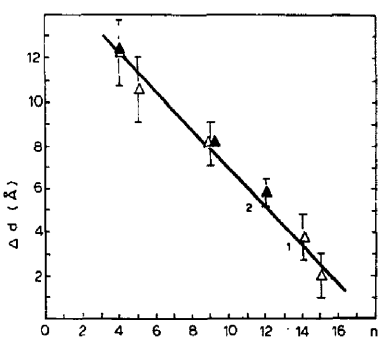

Fig. 5. The distance between the bilayer centre and the projections of labelled CH_2-groups on the bilayer normal direction in dependence on the label positions in acyl chains [3,27]: 1, DPPC, 25 wt% H_2O, 50 °C; 2, DPPC, 10 wt% H_2O, 70 °C.

spin-labels do not allow use of labeled lipids for quantitative measurements of the molecular conformations. Our experimental conditions are similar enough to those of Refs. 4 and 27 at 25 wt% H_2O and it is reasonable to take the same angle of the segment tilting, $\phi = 44°$.

It is interesting that the same value can be calculated from the ratio of the area of the phosphatidylcholine head group A_0 and of two chain cross-sections $2a_0$, assuming that the excess headgroup area can be compensated by the chain tilting when they are closely packed. If $A_0 = 59$ Å^2 [36] and $2a_0 \cong 40$ Å^2 [14], $\phi =$ arc cos$(2a_0/A_0) \cong$ arc cos $0.69 \cong 45°$. Thus i-defects are triangular in form. It is reasonable to suppose that the defects of 2Δ and Δ width (Fig. 4) are equally probable (they depend on the mutual orientation of the planes in which the chain bending takes place). If the triangle side is the 'segment' of approx. 10 Å length (8 CH_2-groups)and $\phi = 44°$, the defect width is $\Delta \cong 7$ Å or $2\Delta \cong 14$ Å and the depth $l_d \cong 7.2$ Å. The respective cross-section areas, S_c, are 25 or 50 Å^2.

Let us suppose for simplicity that a cluster is surrounded by the 'average' annular defect with $S_c = 0.5(25 + 50) = 37$ Å^2. The average triangle base is $\frac{3}{2}\Delta \cong 10.5$ Å and the annulus diameter is approx. R_g. The effective diameter of the lipid 'core' (two cluster diameters):

$$D_c \cong 2R_g - (3/2)\Delta \cong 48 \text{ Å}$$

Thus the minimal size of a cluster along the bilayer surface $r_c = D_c/2 = 24$ Å, which correlates with Segerman's estimations [29]. A part of i-defect area is screened by lipid polar groups against water. The volume and the surface area of the defect can be calculated from the above geometric notions and the defect concentration can be determined from Eqn. 1. The parameters of i-defects in liquid-crystalline phosphatidylcholine bilayers are given in Table IV, taking into consideration the multibilayer repeat distance $d = 54$ Å.

If the fraction of the bilayer area occupied by defects is known, the permeation of water through such a clustered bilayer can be roughly estimated, suggesting that only the central 'disordered' hydrocarbon layer (see Fig. 4) acts as a diffusion barrier and the defects (but not the clusters) are fully permeable for water and other molecules and ions. Permeability was measured for liposomes (see above). At maximum hydration the DPPC and EPC bilayers have the hydrocarbon interior thickness $l_h \cong 26$ Å [14] and taking into account the thickness of two clustered layers (approx. 14 Å), the thickness of a central 'disordered' layer $l \cong 12$ Å. Supposing its properties to be similar to those of liquid paraffins, the permeability coefficient, P, can be calculated as:

$$P = \alpha_S \frac{KD}{l} \tag{5}$$

TABLE IV

Parameters of i-defects in liquid-crystalline DPPC bilayers at 97% relative humidity and 55°C

Parameters of defects	Formula	Value
Ground width	$(3/2)\Delta$	10.5 Å
Depth	l_d	7.2 Å
Cross-section area	$S = (3/4)\Delta \cdot l_d$	37 Å^2
Radius of an annular defect	$R = R_g$	29 Å
Area at the bilayer surface	$S_d = 3\pi R \cdot \Delta$	$1.9 \cdot 10^3$ Å^2
Volume	$V_d = 2\pi R S_c$	$6.7 \cdot 10^3$ Å^3
Total concentration	$n = \frac{I(0)}{(\rho - \rho_S)^2 V_d^2}$	$1.7 \cdot 10^{18}$ cm^{-3}
Fraction of the total sample volume occupied by defects	$\alpha_V = nV_d$	$1.14 \cdot 10^{-2}$
Number of defects per 1 cm^2 of a bilayer surface	$n_S = \frac{nd}{2}$	$4.6 \cdot 10^{11}$
Fraction of a bilayer area occupied by defects	$\alpha_S = n_S S_d$	0.088

where α_S is given in Table IV, K is the partition coefficient between aqueous and hydrocarbon phases and D is the diffusion constant. For water molecules in liquid hexadecane $D \cong 2 \cdot 10^{-5}$ cm$^2 \cdot$ s^{-1} and $K = 4.2 \cdot 10^5$. The substitution of these values into Eqn. 5 gives $P \cong 1.7 \cdot 10^{-3}$ cm $\cdot$ s^{-1} i.e., it is of the same order as the experimental one [65].

Clusters: chain packing and dimensions

An average cluster diameter along the DPPC bilayer plane $R_c \cong 24$ Å at 55°C and 97% RH as it was calculated above. By independent methods this value was estimated in Refs. 15, and 35 for various lipids from the halfwidth of (4.6 Å)$^{-1}$ diffuse X-ray reflex. It the instantaneous chain distribution respective to the average positions is described by the Gaussian function [78], the correlation radius equal to the cluster minimal dimension is obtained:

$$R_c \cong \frac{1.6h^2}{\Delta q'_{1/2}} \tag{6}$$

where h is the order of the Bragg reflex, $\Delta q'_{1/2}$ is its half-width [15,35] ($q' = q/2\pi$).

At maximum hydration $R_c = 28$ Å for DPPC at 45°, 29 Å for azolectin and 27 Å for egg PC at 20°C; for 'dry' lipid bilayers this value decreased to 19–22 Å [35].

Thus, the cluster dimensions are of the same order * in comparison with that obtained by small angle neutron scattering.

The 'packing' reflex at $q' = (4.6\ \text{Å})^{-1}$ is, apparently, not the Bragg reflection for the quasicrystalline lattice of the hexagonal symmetry as some authors suggested [11,51–53] and the chain melting is not the lattice 'swelling'. The peak position rather reflects the average interchain separation at the close packing of chains. It is determined by the chain cross section [14,15,35] analogously to liquid paraffins [28,78]. The correlation radius (cluster dimension) reflects the short-range order of the molecular arrangement. It gives the coefficient 1.6 in Eqn. 6.

From the position of the 'packing' reflex can be calculated the average interchain distance and the average cross-section area of the single chain in the cluster. For closely packed chains undergoing 'statistical rotation' around their long axes, the scattering centre distribution can be proposed as the superposition of two virtual hexagonal lattices with the closest and for the 'friable' chain packing [78]. The peak maximum corresponds to the distance:

$$r = \tfrac{1}{2}(r_{\min} + r_{\max}) \cong 4.65\ \text{Å} \tag{7a}$$

where $r_{\min} = 4.1$ Å and $r_{\max} = 5.2$ Å are taken from the cross-section form of a chain [14,15,35,78].

The virtual lattice with the closest packing corresponds to the solid (gel) state, and the average cross-section area is $a_g \cong 4.1^2/\sin 60° = 19.4\ \text{Å}^2$. For free rotating chains (the 'friable' lattice) the peak maximum corresponds to the neighbouring chain separation analogously to liquids, and the cross-section area, a_l, can be calculated as $a_l \cong 5.2^2 \sin 60° = 23.4\ \text{Å}^2$. The average area per chain can be calculated as a mean for these two 'quasilattices':

$$a_0 = \tfrac{1}{2}(a_g + a_l) \cong 21.4\ \text{Å}^2 \tag{7b}$$

This value calculated from only the position of X-ray reflex can be compared to an estimation obtained on the basis of other data. The average volume of the CH_2-group in liquid-crystalline phosphatidylcholine bilayers is equal to about 27 Å^3 [23]. The average cross-section area of a chain is, consequently, $a_0 \cong 27/1.25 = 21.6\ \text{Å}^2$. Other estimations can be made from the values of the head-group area, A_0 at a bilayer surface and the angle of the chain tilt, ϕ. If the closely packed chains are tilted to compensate the excess area of a polar head group the single chain cross-section area is

$$a_0 = \tfrac{1}{2} A_0 \cos\phi \tag{8}$$

analogously to the procedure for $L_{\beta'}$-phase [18]. For $A_0 = 59.2$ Å^2 [36] and $\phi = 44°$, as was shown above, the a_0 value is 21.3 Å^2.

Thus three different approaches give similar values. From the average cross-section area of a chain, the average chain separation value can be found (it can not be calculated directly from the reflex position). In a solid bilayer characterized by the reflex $(4.1\ \text{Å})^{-1}$, the interchain separation $r_{hc} = 4.1/\sin 60° = 4.75$ Å. If the area ratio is proportional to the square of the interchain separation ratio, the average distance between adjacent chains is

$$\bar{r}_{hc} = 4.75\sqrt{a_0/a_g} = 4.75\sqrt{21.4/19.4} \cong 5.0\ \text{Å} \tag{9}$$

According to Ref. 79 the critical separation for generation of the *gauche* conformation is more than 4.9 Å. Petersen and Chan [49] estimated the probability of all-*trans*-conformers for the C1-C9 'segments' of chains as $1.0 \geqslant \rho_t \geqslant 0.8$ in liquid phosphatidylcholine bilayers. Thus the clustered chains may have some number of *gauche* conformers (for example one kink per 'segment').

The alternative estimations of the interchain separation assume that the phase transition from a solid to a liquid bilayer results only in the 'swelling' of the hexagonal chain lattice. This is reflected as the Bragg maximum displacement from $(4.1\ \text{Å})^{-1}$ to $(4.6\ \text{Å})^{-1}$ with long-range order preservation [11,45,67]. Then the average distance between the adjacent chains is equal to 5.21 Å [53], 5.3 Å [11] or 5.56 Å [12]. The average area per phosphatidylcholine molecule is respectively 47–50 Å^2 [53], which is significantly less than the 60–70 Å^2 obtained from the experimental data [11,14,15,17].

The difference between the average area per molecule at the bilayer surface and the area of the hydrated polar head-group is determined by the area of defects between clusters. In this case for $d = 54$ Å, 25 wt% H_2O (we can use the data in Refs. 4 and 27) and the partial specific DPPC volume of approx. 1 ml · g^{-1}, the average area per molecule, calculated according to Ref. 17, is equal to 62–63 Å^2, i.e., 4.8–6.4% of the bilayer surface is occupied by defects. This value is less than that in Table IV, which can be explained by the partial 'screening' of the defect surface by the lipid head-groups.

Chain packing and motion

The thickness of two clustered layers is about 14 Å. If the repeat distance is approx. 54 Å, their fraction in the sample volume is about 26%. Then the i-defects occupy approx. 1.14% of the total sample volume and

* It is necessary to emphasize that a wrong estimate of the cluster minimal dimension was made in Ref. 25, where the value $2r_c$ was used instead of r_c.

approx. 4% of the volume of two clustered layers, because they are located exclusively in the clustered layers. The topology of a bilayer assumes that the inner m-defects also occupy approx. 4% of the clustered layer volume. Taking into consideration the clustered layer thickness and the average area per molecule, the volume of the ordered part of a phosphatidylcholine molecule (a 'clustered' part) is about 450 Å^3 and the defect volume is about 18 Å^3 per DPPC molecule.

The density of a central 'disordered' layer can be easily calculated. Bilayer geometry suggests that the volume of the more disordered part of DPPC molecule (C10–C16 groups) is equal to about 450 Å^3. Its molecular mass is 198 and the effective density $\rho \cong 0.735$ g · cm^{-3}, i.e., it is equal to the density of tetradecan at 55°C (approx. 0.74 g · cm^{-3}). Thus the DPPC hydrocarbon interior at 55°C and 97% RH can be imagined as a 'sandwich' of two clustered layers adjacent to the polar regions and the central liquid (disordered) layer with its density identical to the tetradecan.

There is extensive information on the lipid molecule dynamics in lipid bilayers [5–8,10,18,20,22,26,43–46,49,50,80–83] but at present it is impossible to describe unequivocally the whole chain motion. Nevertheless, it is reasonable to suggest that the 'plateau' in ^{2}H and ^{13}C NMR spin-relaxation time and order parameter profiles should be determined by the cluster organization of a bilayer, and the axial symmetry of the molecule motion is in the main a result of the cluster reorientation relative to the local bilayer normal. The characteristic time of chain reorientation about the normal direction of approx. 10^{-7} s was estimated by Petersen and Chan [49]. For ESR lipid spin-probes the correlation time of long-axis reorientation, $\tau_{R\perp}$, is about $6.1 \cdot 10^{-8}$ s (23°C, DMPC) and $1.3 \cdot 10^{-8}$ s (50°C, DMPC) [8].

These values are close to those for ultrasonic relaxation: approx. $2.1 \cdot 10^{-8}$ at 44°C and approx. $1.5 \cdot 10^{-8}$ s at 47°C in DPPC bilayers [82]. Indeed, the cluster lifetime, τ_1, can not be larger than the time, τ_D, needed for a lipid molecule to diffuse from the centre to cluster boundary, i.e.,

$$\tau_1 < \tau_D \cong R^2/4D$$

where R is the cluster radius, D is the lateral diffusion constant for lipid molecules. For $R = 12$ Å and $D = 2 \cdot 10^{-8}$ cm$^2 \cdot$ s^{-1} the value $\tau_D \cong 1.8 \cdot 10^{-7}$ s.

The existence of m-defects can explain, apparently, the strange fact of the very large vertical fluctuations of chains in a liquid bilayer which were detected by double electron-electron resonance of the ^{14}N and ^{15}N labelled lipid probes [84], by double nuclear magnetic resonance (proton-enhanced ^{13}C-NMR) [25] and by dynamic quenching of the fluorescent labels [85]. The time-scale range of these processes is approx. 10^{-8} s judging by the lifetime of the label excited state [85].

The large wobbling amplitude for the membrane fluorescent probe motion in the nanosecond time scales [12,86] can be also explained by the probe location in defects, outer or inner depending on the probe molecular structure.

Conclusion

Small-angle neutron scattering in the direction parallel to the bilayer surface shows the existence of inhomogeneities with the average gyration radius of approx. 29 Å. It is reasonable to interpret them as the water-contrasted intercluster defects. A clustered molecular arrangement is apparently a general feature of liquids and liquid-crystals [28,85] and was suggested earlier for lipid bilayers and membranes [15,16,17,29,30,35] to explain the X-ray scattering and the behaviour of molecular probes. Analysis of numerous experimental data suggests that clusters are formed by the hydrocarbon chain all-*trnas*-segments of about 8 CH_2-groups in length. Their tilt to the bilayer surface is determined by the lipid head-group area and it changes with head-group hydration. Such structural organization leads to close chain packing and maximum molecular interactions in the hydrocarbon region of a bilayer.

Thus the bilayer hydrophobic interior can be imagined as a three layer 'sandwich' with the more disordered 'liquid' layer in its centre. The thickness of a clustered layer is about 7 Å and its permeability for molecules and ions is determined by the average area of defects at the bilayer surface and by the thickness of the central disordered layer that is similar to the liquid hydrocarbon layer.

Cluster dimensions along the DPPC bilayer surface were estimated to the approx. 24 Å by the small-angle scattering method and from the halfwidth of the X-ray 'packing' reflex (4.6 Å)$^{-1}$. The average cross-section area per a hydrocarbon chain in a cluster was estimated approx. 21.4 Å^2 from the reflex position and chain cross-section geometry with respect to the interchain separation of approx. 5 Å. The average volume of the i-defect at the bilayer interface is estimated to be approx. 18 Å^3 per DPPC molecule. A cluster model explains the numerous experimental data and does not, in principle, contradict the recent theoretical presentations.

References

1 Singer, S.J. (1974) Annu. Rev. Biochem. 43, 805–833.
2 Abrahamsson, S., Dahlen, B., Löfgren, H., Pascher, I. and Sundell, S. (1976) in Structure of Biological Membranes (Abrahamsson, S. and Pascher, I., eds.), pp. 1–23, Plenum, New York.
3 Büldt, G., Gally, H.U., Seelig, J. and Zaccai, G. (1979) J. Mol. Biol. 134, 673–691.

4 Büldt, G., Gally, H.U., Seelig, A., Seelig, J. and Zaccai, G. (1978) Nature 271, 182–184.
5 Cullis, P.R., De Kruijff, B., McGrath, A.E., Morgan, C.G. and Radda, G.K. (1977) in Structure of Biological Membranes (Abrahamsson, S. and Pascher, I., eds.), pp. 389–407, Plenum, New York.
6 Davis, J.H. (1979) Biophys. J. 27, 339–358.
7 Davis, J.H. (1983) Biochim. Biophys. Acta 737, 117–171.
8 Davis, J.H. (1986) Chem. Phys. Lipids 40, 223–258.
9 Edhalm, O., Nilsson, L., Berg, O., Ehrenberg, M., Claerens, F., Graslund, A., Jönsson, B. and Teleman, O. (1984) Q. Rev. Biophys. 17, 125–151.
10 Fuson, M.M. and Prestepard, J.H. (1983) Biochemistry 22, 1311–1316.
11 Hauser, H., Pascher, I., Pearson, R.H. and Sundell, S. (1981) Biochim. Biophys. Acta 650, 21–51.
12 Ikegami, A., Kinosita, K. and Kouyama, T. (1982) in Structure, dynamics and Biogenesis of Biomembranes, pp. 1–31, Plenum, New York; Japan Scientific Societies Press, Tokyo.
13 Israelachvili, J.M., Marcelja, S. and Horn, R.G. (1980) Q. Rev. Biophys. 13, 121–200.
14 Ivkov, V.G. and Berestovsky, G.N. (1981) Dynamic Structure of a Lipid Bilayer, pp. 1–292, Nauka, Moscow (in Russian).
15 Ivkov, V.G. and Berestovsky, G.N. (1982) Lipid Bilayer of Biological Membranes, pp. 1–224, Nauka, Moscow (in Russian).
16 Bashford, C.L., Morgan, C.G. and Radda, G.K. (1976) Biochim. Biophys. Acta 426, 157–172.
17 Levine, Y.K. (1972) Progr. Biophys. Membr. Struct. 24, 1–74.
18 Levine, Y.K., Birdsall, N.J.M., Lee, A.G. and Metcalfe, Y.C. (1972) Biochemistry 11, 1416–1421.
19 Seelig, A. and Seelig, J. (1974) Biochemistry 13, 4839–4845.
20 Seelig, J. (1977) Q. Rev. Biophys. 10, 353–418.
21 Seelig, J. (1981) in Membranes and Intercellular Communications (Balian, R. et al., eds.), pp. 17–78, North-Holland, Amsterdam.
22 Seelig, J. and Seelig, A. (1980) Q. Rev. Biophys. 13, 19–61.
23 Tardieu, A., Luzzati, V. and Reman, F.C. (1973) J. Mol. Biol. 75, 711–734.
24 Worcester, D.L. and Franks, N.P. (1976) J. Mol. Biol. 100, 359–378.
25 Xu, Z.-C. and Cafiso, D.C. (1986) Biophys. J. 49, 779–783.
26 Yeagle, P.L. and Frye, J. (1987) Biochim. Biophys. Acta 899, 137–172.
27 Zaccai, G., Büldt, G., Seelig, A. and Seelig, J. (1979) J. Mol. Biol. 134, 693–706.
28 Stewart, G.W. (1928) Phys. Rev. 31, 174–181.
29 Segerman, E. (1968) in Membrane Models and the Formation of Biological Membranes (Bolis, L. and Pethica, B.A., eds.), pp. 52–75, North-Holland, Amsterdam.
30 Lee, A., Birdsall, N.J.M., Metcalfe, J.C., Toon, P.A. and Warren, G.B. (1974) Biochemistry 13, 1695–1705.
31 Rubinshtein, D.L. (1947) General Physiology, Medgiz, Moscow (in Russian).
32 Jain, M.K. (1983) in Membrane Fluidity in Biology, Vol. 1, Concepts of Membrane Structure (Aloin, R.C., ed.), pp. 1–37, Academic Press, New York.
33 Deamer, D.W. and Bramhall, J. (1986) Chem. Phys. Lipids 40, 167–188.
34 Traüble, H. (1971) J. Membr. Biol. 4, 193–208.
35 Ivkov, V.G., Kazakov, V.A. and Kornev, A.N. (1984) Biofizika 29, 410–414.
36 Ivkov, V.G. (1986) Biofizika 31, 784–788.
37 Ivkov, V.G. (1986) Biofizika 31, 245–251.
38 Epand, R.M. and Epand, R.F. (1980) Chem. Phys. Lipids 27, 139–150.
39 Melchior, D.L. and Morowitz, H.J. (1972) Biochemistry 11, 4558–4562.
40 Nagle, J.F. and Wilkinson, D.A. (1978) Biophys. J. 23, 159–175.
41 Allegrini, P.R., Van Scharrenburg, G., DeHaas, G.H. and Seelig, J. (1983) Biochim. Biophys. Acta 731, 448–455.
42 Boden, N., Jackson, P., Levine, Y.K. and Ward, A.J.I. (1976) Biochim. Biophys. Acta 419, 395–403.
43 Brown, M.F., Ribeiro, A.A. and Williams, G.D. (1983) Proc. Natl. Acad. Sci. USA 80, 4325–4329.
44 Davis, J.H. and Jeffrey, K.R. (1977) Chem. Phys. Lipids 20, 87–104.
45 Lee, A., Birdsall, N.J.M., Metcalf, J.C., Warren, G.B. and Roberts, G.C.K. (1976) Proc. R. Soc. London B193, 253–274.
46 Marsh, D., Watts, A. and Smith, C.P. (1983) Biochemistry 22, 3023–3026.
47 McLaughlin, A.C., Podo, F. and Blasie, J.K. (1973) Biochim. Biophys. Acta 330, 109–121.
48 Pace, R.J. and Chan, S.I. (1982) J. Chem. Phys. 76, 4217–4228.
49 Petersen, N.O. and Chan, S.I. (1977) Biochemistry 16, 2657–2667.
50 Reeves, L.W. and Tracey, A.S. (1975) J. Am. Chem. Soc. 90, 5729–5735.
51 Brady, G.W. and Fein, D.B. (1977) Biochim. Biophys. Acta 464, 249–259.
52 Marsh, D. (1974) J. Membr. Biol. 18, 145–162.
53 Ruocco, M.J. and Shipley, G.G. (1982) Biochim. Biophys. Acta 691, 309–320.
54 Vogel, H. and Jähnig, F. (1981) Chem. Phys. Lipids 29, 83–101.
55 Balagurov, A.M., Gordeliy, V.I. and Yaguzhinskiy, L.S. (1986) Biofizika 31, 31–34.
56 Powers, L. and Pershan, P.S. (1977) Biophys. J. 20, 137–152.
57 Vagov, V.A., Kunchenko, A.B., Ostanevich, Yu.M. and Salamatin, I.M. (1983) in Communications of the Joint Institute for Nuclear Research, p. 14-83-896, Dubna (in Russian).
58 Bezzabotnov, V.Yu, Gordeliy, V.I., Ostanevich, Yu.M. and Yaguzhinskiy, L.S. (1987) in Communications of the Joint Institute for Nuclear Research, p. 14-87-88, Dubna (in Russian).
59 Svergun, D.I. and Feigin, L.A. (1986) X-Ray and Neutron Small-Angle Scattering, Nauka, Moscow (in Russian).
60 Jendrasiak, G.L. and Hasty, J.H. (1974) Biochim. Biophys. Acta 337, 79–91.
61 Katchalsky, A., Kedem, O., Klibonsky, C. and De Vries, A. (1960) in Flow Perspectives of Blood and Other Biological Systems, p. 155, Pergamon, New York.
62 Markin, V.S. and Kozlov, M.M. (1985) Biol. Membr. 2, 205–223 (in Russian).
63 Andersen, O.S. (1978) in Membrane Transport in Biology, Vol. 1, Concepts and Models (Giebisch, et al., eds.), pp. 369–446, Springer, Berlin.
64 Main Formulae of Physics (1957) p. 607, Nauka, Moscow.
65 Peterson, D.C. (1977) Biochim. Biophys. Acta 16, 2657–2667.
66 Cooke, R. and Kuntz, I.D. (1974) Annu. Rev. Biophys. Bioeng. 3, 95–125.
67 Fettiplace, R. and Haydon, D.A. (1980) Physiol. Rev. 60, 510–550.
68 Katz, Y., Hoffman, M.E. and BLumenthal, R. (1983) J. Theor. Biol. 106, 493–510.
69 Vodyanoy, I. and Hall, J.E. (1984) Biophys. J. 29, 187–194.
70 Schindler, H. and Seelig, J. (1975) Biochemistry 14, 2283–2287.
71 Gruen, D.W.R. (1985) J. Phys. Chem. 89, 146–153.
72 Gruen, D.W.R. (1985) J. Phys. Chem. 89, 153–163.
73 Marcelja, S. (1974) Biochim. Biophys. Acta 367, 164–176.
74 Birrell, G.B. and Griffith, O.H. (1976) Arch. Biochem. Biophys. 172, 455–462.
75 Grower, A.K., Forrest, B.J., Buchinski, R.K. and Cushley, R.J. (1979) Biochim. Biophys. Acta 550, 212–221.
76 McFarland, B.G. and McConnell, H.M. (1971) Proc. Natl. Acad. Sci. USA 68, 1274–1278.
77 Ohki, S. and Ohki, C.B. (1976) J. Theor. Biol. 62, 389–407.

78 Vainstein, B.K. (1963) X-ray Diffraction on Chain Molecules, Nauka, Moscow (in Russian).
79 Bothrel, G.W., Belle, J. and Lemaire, B. (1974) Chem. Phys. Lipids 12, 96–116.
80 Cornell, B.A. and Pope, J.M. (1980) Chem. Phys. Lipids 27, 151–164.
81 Galla, H.-J., Hartmann, W., Theilen, U. and Sackmann, E. (1979) J. Membr. Biol. 48, 215–236.
82 Mitaku, S. and Date, T. (1982) Biochim. Biophys. Acta 688, 411–421.
83 Vogel, H. and Jähnig, F. (1985) Proc. Natl. Acad. Sci. USA 82, 2029–2033.
84 Feix, J.B., Popp, C.A., Venkataramy, S.D., Beth, A.H., Park, J.H. and Hyde, J.S. (1984) Biochemistry 23, 2293–2299.
85 Frenkel, Ya.I. (1975) Kinetic Theory of Liquids, Nauka, Leningrad (in Russian).